Radial Size of a Starburst Dendrimer in Solvents of Varying Quality

Yu-Jane Sheng,[†] Shaoyi Jiang,[‡] and Heng-Kwong Tsao*[,§]

Department of Chemical Engineering, National Taiwan University, Taipei, Taiwan 106, Republic of China; Department of Chemical Engineering, University of Washington, Box 351750, Seattle, Washington 98195-1750; and Department of Chemical and Materials Engineering, National Central University, Chung-li, Taiwan 320, Republic of China

Received May 28, 2002
Revised Manuscript Received September 2, 2002

A starburst dendrimer that resembles a Cayley tree is a regularly branched polymer with a starlike cascade topology. They have shown promise as vehicles of controlled-release systems and as molecular scaffolds for chemical catalysts.[1] Dendrimers are characterized by the branch-juncture multiplicity b, the number of monomer segments P between the functional groups (the spacer), and the number of generation g they contain. Despite the fact that the maximum accessible volume only increases cubically with the number of generation, $\sim[(g+1)P]^3$, the volume occupied by the starburst in a space-filling state grows exponentially with the generation, $\sim P(b-1)^{g+1}$. Because the accessible volume grows slower than the occupied volume with increasing generation, a perfect dendrimer can be grown up to a limiting generation number, $g_m \sim \ln[P(l^3)/v]]$. Here l and v are respectively the length and the excluded volume of the monomer segment.

The success of the scaling theory for a linear chain in a dilute solution is well-known. It predicts that a universal scaling exponent exists for the polymer size.[2] For a regularly branched polymer like a dendrimer, however, currently there is a controversy in the literature as to the dependence of the radial size on the number of segments. An early attempt to investigate the structure of dendrimers was made by de Gennes and Hervet.[3] They employed a self-consistent mean-field analysis based on the assumption that the monomers of each generation lie in a concentric shell of their own. With long spacers, they found that the size of the dendrimer was proportional to $N^{1/5}P^{2/5}$, with N being the total number of monomers. Lescanec and Muthukumar[4] built dendrimers based on an off-lattice kinetic growth algorithm of self-avoiding walk. In their simulations, significant chain folding is observed, and the density profile decreases outward from the center of the dendrimer monotonically. The dendrimer size is scaled as $N^{0.22}P^{0.5}$. Mansfield and Klushin[5] performed Monte Carlo (MC) calculations on a diamond lattice. They found that the density profile is qualitatively similar to that found in ref 4, and the terminal groups are dispersed throughout the molecule. Chen and Cui[6] proposed a scaling law, $(P_g)^{1-\nu}N^{2\nu-1}$, for large g. Their MC results imply that the scaling exponent ν for a starburst dendrimer has the same value as that of a linear polymer.

The dendrimers for all aforementioned studies were in a very good solvent and in the dilute limit. Murat and Grest[7] performed molecular dynamics (MD) simulations under varying solvent conditions. They predicted a compact structure under all solvent condition, with a dendrimer size proportional to $N^{1/3}$. Recently, the dimension of the poly(propyleneimine) dendrimers, as measured by both SANS and viscosimetry, increases roughly as $M^{1/3}$, where M is the molar mass of the dendrimer.[8] This relationship proves to be independent of the solvent used. These results are in line with the MD study of ref 7. Although the nature of the intramolecular density profile and the position of the terminal groups have been better understood, the exact scaling of the radial size associated with a dendrimer is still the source of some controversy. In this Communication, we confirm the scaling predicted by the Flory-type theory using MC simulations.

Ideally, flexible dendrimers access all configurations to maximize the conformation entropy, which can be estimated by the phantom dendrimer. For a freely jointed phantom starburst, the mean-square center-to-end distance is simply $R_{e,0}^2/\langle l\rangle^2 = (g+1)P$. The mean-square radius of gyration can also be obtained analytically.[9,10] For $b = 3$, one has

$$\frac{R_{g,0}}{\langle l^2\rangle}N^2 = 3P^3\{-1 + 6\cdot 2^{g+1} + [3(g+1)-5]2^{2(g+1)}\} - \frac{P(P-1)}{2}(2^{g+1}-1)(9\cdot 2^{g+1}P - 7P + 2) \quad (1)$$

where the total number of vertexes is $N = 3P(2^{g+1}-1) + 1$. For $2^{g+1} \gg 1$ and $P \gg 1$, $R_{g,0}^2/\langle l^2\rangle \approx P[g - {}^7/_6 + (2g + {}^5/_9)/2^{(g+1)}] + {}^1/_2$. This exploration of phase space results in a "dense core" dendritic structure.[9] Note that for a selected generation the size of a phantom dendrimer grows just like a Gaussian chain, $R_{g,0} \propto N^{1/2}$, as the spacer length is increased. The subscript "0" denotes a phantom dendrimer.

The segment−segment interactions including excluded volume and van der Waals attraction, however, can accommodate the entropic penalty for swelling or compressing the molecule from its preferred Gaussian configurations. Following the generalized Flory-type theory for a linear chain,[2] the free energy for *a single linear branch of (g + 1)P segments in the starburst* is given by[9]

$$\frac{F}{kT} \approx \left(\frac{R_g}{R_{g,0}}\right)^2 + \left(\frac{R_{g,0}}{R_g}\right)^2 + (g+1)PB\left(\frac{N}{R_g{}^3}\right) + (g+1)PC\left(\frac{N}{R_g{}^3}\right)^2 \quad (2)$$

The first two terms represent the elastic deformation of entropic nature and correspond to the extension and compression, respectively. They are the elastic energy associated with a linear branch of a dendrimer based on similar expressions for a linear chain. The total elastic energy can be obtained by multiplying the two terms by a factor $N/(g+1)P$, which is the number of

[†] National Taiwan University.
[‡] University of Washington.
[§] National Central University.
* To whom correspondence should be addressed: e-mail hktsao@cc.ncu.edu.tw.

10.1021/ma025561k CCC: $22.00 © 2002 American Chemical Society
Published on Web 09/13/2002

linear branches within a dendrimer. The third and fourth terms denote the segment−segment interactions. $B \sim v$ and $C \sim v^2$ are the second and third virial coefficients, respectively. The total interaction energy for a dendrimer can be obtained by replacing $(g + 1)P$ with N. The total free energy of a dendrimer is equivalent to that of a linear branch times the factor $N/(g + 1)P$.

The equilibrium size in terms of the linear expansion factor ($\alpha = R_g/R_{g,0}$) is determined from the condition of the minimum for the total free energy

$$\alpha^5 - \alpha^1 \approx (g + 1)PR_{g,0}{}^{-3}NB + (g + 1)PR_{g,0}{}^{-6}N^2C\alpha^{-3} \quad (3)$$

When $\alpha^4 \gg 1$ (in a good solvent), the repulsion between the segments dominates, and one obtains

$$R_g \sim N^{1/5}(g + 1)^{2/5}P^{2/5} \quad (4)$$

It is remarkable that eq 4 is similar to the result of ref 3. Nonetheless, the latter concluded that the polymer volume fraction grows parabolically near the core and reaches its limiting value 1 at the outer regions, a "dense shell" structure. Equation 4 coincides with the conjecture in ref 6 and indicates a limiting generation number because the fractal dimensionality is greater than 3. In fact, eq 4 is the same spacer scaling derived and demonstrated in ref 9. On the other hand, as $\alpha \ll 1$, the attraction prevails, and the size of a dendrimer is simply given by

$$R_g \sim N^{1/3} \quad (5)$$

It is simply indicative of a compact (space-filling) structure.

To confirm the scaling, we perform off-lattice MC simulations in both good and poor solvent conditions. The dendrimer is modeled as a freely jointed, square-well dendritic chain. The nonbonded beads i and j interact via a square-well potential

$$\begin{aligned} U_{ij}(r) &= \infty, \quad r < \sigma \\ &= -\epsilon, \quad \sigma < r < 1.5\sigma \\ &= 0, \quad r > 1.5\sigma \end{aligned} \quad (6)$$

where σ is the bead hard-core diameter.

Bonded beads i and $i + 1$ interact via an infinitely deep square-well potential[11]

$$\begin{aligned} U_{i,i+1}(r) &= \infty, \quad r < \sigma \\ &= 0, \quad \sigma \le r \le 1.4\sigma \\ &= \infty, \quad r > 1.4\sigma \end{aligned} \quad (7)$$

Each randomly selected bead on the dendritic polymer was allowed to move around its position with a restriction of the bond fluctuation between σ and 1.4σ. In this Communication, we present MC simulations for $g = 1-7$ with P varying from 1 to 50. The number of MC steps per bead is more than 10^6. The mean-square bond length is $\langle l^2 \rangle \approx 1.51\sigma^2$ in the athermal condition. The radius of gyration of a phantom dendrimer calculated by MC simulations agrees excellently with that predicted by eq 1.

Figure 1 shows that the radius of gyration associated with an athermal dendrimer for a specified spacer length can be mistakenly fitted by the power law $N^{1/3}$. Here R_g is defined as the root of mean-square monomer−center distance. This outcome agrees with those obtained by MD[7] and experiments.[8] As the spacer length varies for a chosen generation, however, the radius of gyration can only be represented by $N^{3/5}$ as illustrated in Figure 2. This result is not surprising because the asymptotic behavior for large P is expected to follow the power law associated with a linear chain, N^{ν}. As shown in eq 1, the exponent is $\nu = 1/2$ for a phantom dendrimer. It will be shown later $\nu \approx 1/3$ for a dendrimer in a bad solvent.

To verify the scaling law in good solvents, first, $R_g/(g + 1)^{2/5}$ is plotted against N. As one can see from Figure 3, data for dendrimers of different generations collapse into a single line for a specified P, satisfying the power law $N^{1/5}$. Second, we plot $R_g/P^{2/5}$ vs N. Again,

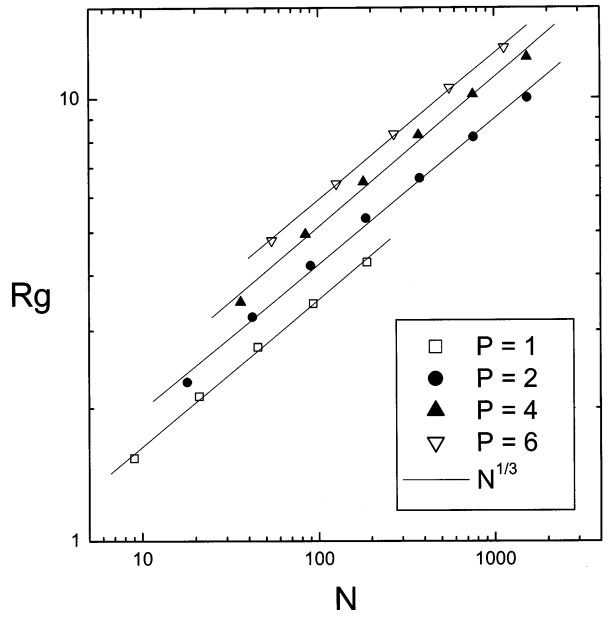

Figure 1. Variation of the radius of gyration R_g with the number of monomers N for different spacer lengths P in a good solvent.

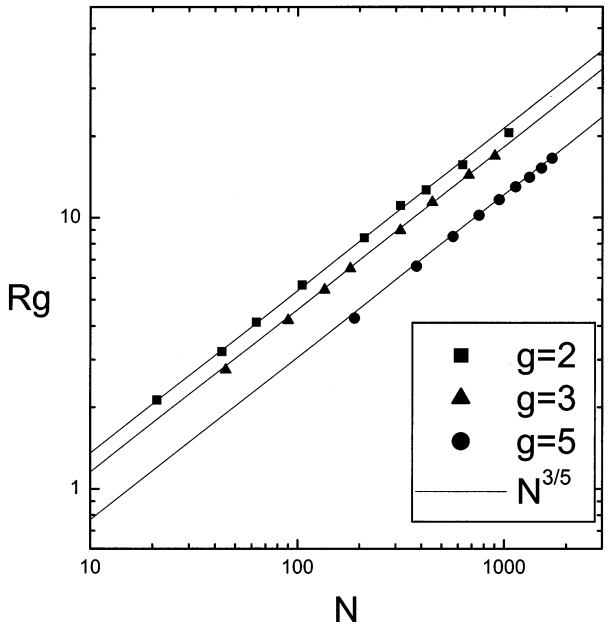

Figure 2. Variation of the radius of gyration with the number of monomers for different generations g in a good solvent.

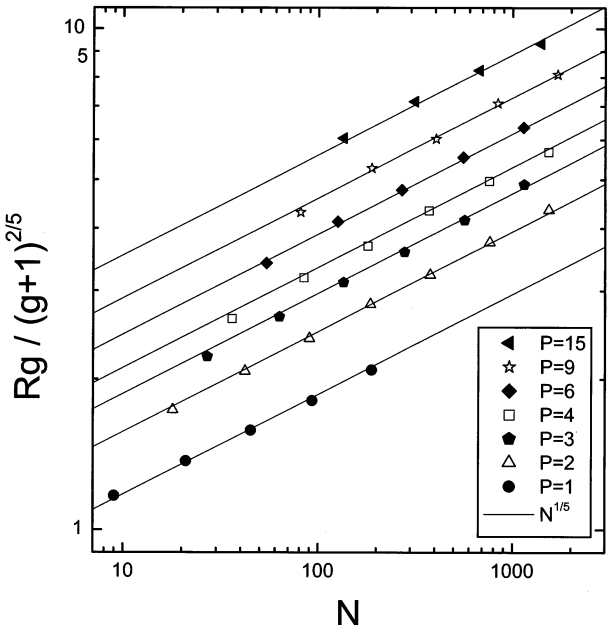

Figure 3. Variation of $R_g/(g + 1)^{2/5}$ with the number of monomers for different spacer lengths.

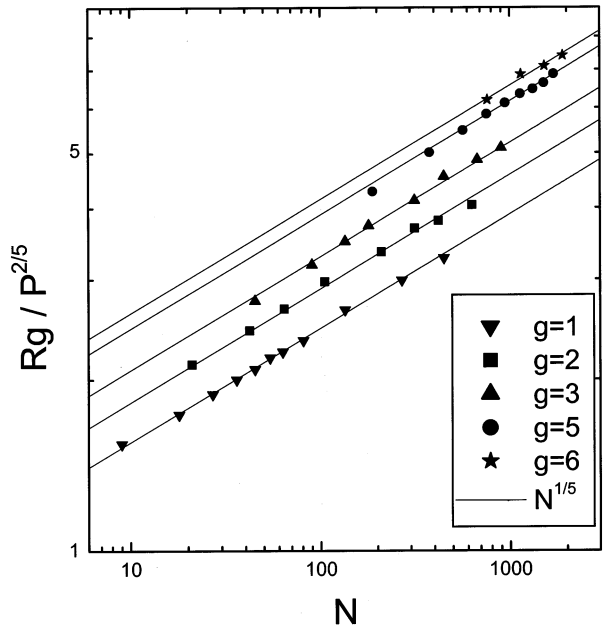

Figure 4. Variation of $R_g/P^{2/5}$ with the number of monomers for different generations.

as depicted in Figure 4, data of different spacer lengths collapse into separate lines with an exponent $^1/_5$ for $g = 2$, 3, and 5. Finally, the effects of both generations and spacer lengths are taken into account in Figure 5. All data for different g and P crumple together in the plot of $R_g/[(g + 1)P]^{2/5}$ against N. The data for $R_g(g,P)$ are listed in Table 1.

The size of a dendrimer falls as the temperature is decreased. Near the θ temperature, the dendritic polymer is believed to behave in a quasi-ideal fashion because of an effective cancellation between the attractive and excluded-volume interactions. Nevertheless, the three-body interactions result in more expanded average structures. The ratio of mean-square radius of gyration to mean-square end-to-end distance of a phantom chain has been proven to be a good criterion for characterizing the θ condition for a linear chain.[12] It fails in this study

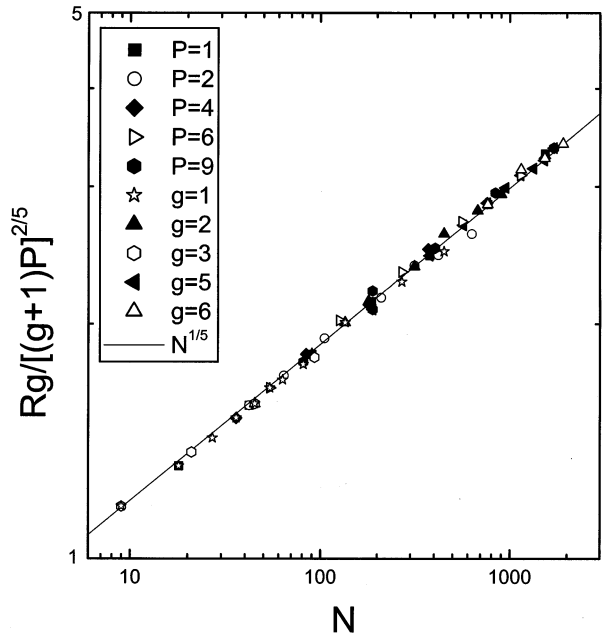

Figure 5. Variation of $R_g/[(g + 1)P]^{2/5}$ with the number of monomers for different values of P and g.

Table 1. Radius of Gyration as a Function of the Spacer Length and the Generation Number[a]

	generation number						
spacer length	1	2	3	4	5	6	7
1	1.54	2.13	2.75	3.45	4.27		
2	2.29	3.22	4.20	5.37	6.61	8.18	10.01
3	2.93	4.13	5.43	6.83	8.50	10.66	
4	3.48	4.94	6.49	8.26	10.19	12.37	
5	3.97	5.66	7.56	9.15	11.65	14.10	
6	4.48	6.42	8.31	10.55	13.00		
7	4.87		8.98		14.10		
8					15.24		
9	5.64	8.24	10.49	13.50	16.57		
10		8.42	11.40	17.76			
15	7.83	11.10	14.38				
20		12.69	16.92				
30	11.65	15.70					
50	15.63	20.60					

[a] The total number of monomers is given by $N = 3P(2^{g+1} - 1)$ for $b = 3$.

because the ratio R_g/R_e for high generation number dendrimers is always greater than that of a phantom chain. Alternatively, since all data collapse into a single curve in the good solvent regime in a plot of $R_g/[(g + 1)P]^{2/5}$ against T^*, one can identify the θ regime, where data of different generations start to separate. According to Figure 6, the dendrimer departs from the good solvent regime as $T^* = (k_BT/\epsilon) \leq 4$. Here k_B is the Boltzmann constant and T is the temperature.

When the temperature is low enough, the dendrimer collapses into compact conformations (poor solvent conditions). It corresponds to the temperature lower than the θ temperature. As shown in Figure 7, the radius of gyration of dendrimers with different g and P is plotted as a function N at $T^* = 1$. All data crumple into a single line with R_g scaled by $N^{1/3}$. This result confirms the scaling behavior, eq 5, in the poor solvent regime. Similar to Figure 6, data of different generations split in the plot of $R_g/N^{1/3}$ against T^* as $T^* \geq 3$. Below this point, all data collapse into a single curve.

For a dendrimer of fixed P in a good solvent regime, R_g can be mistakenly represented by the power law $N^{1/3}$

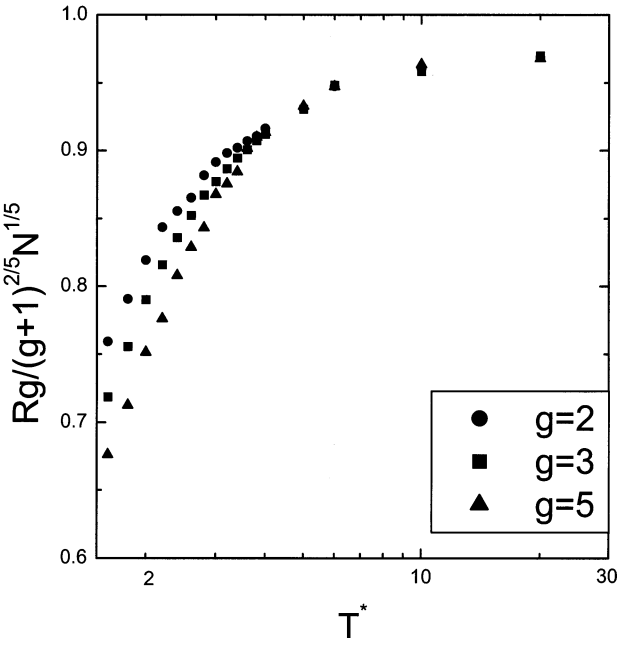

Figure 6. Variation of $R_g/(g + 1)^{2/5}N^{1/5}$ with the scaled temperature T^* for different generations.

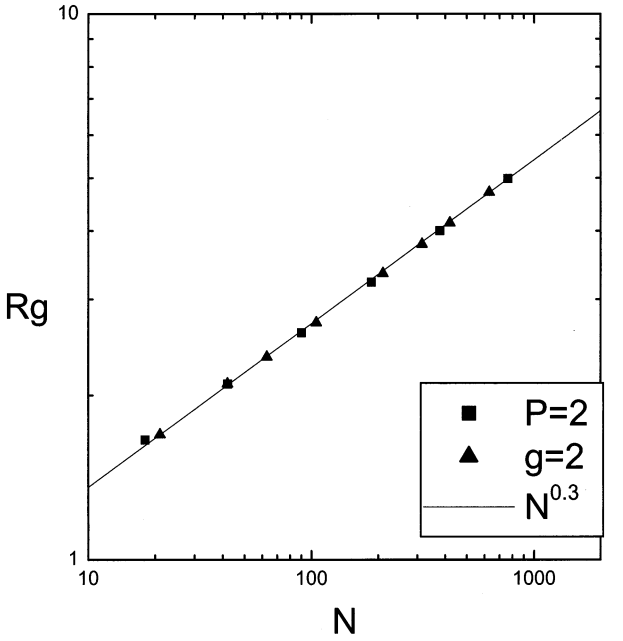

Figure 7. Variation of R_g with the number of monomers for different values of P and g in a poor solvent.

as already demonstrated in Figure 1. On the other hand, R_g should follow the behavior $N^{1/3}$ in the poor solvent. Consequently, one would conclude that the scaling relation of the dendrimer size is independent of the solvent used, that is, the quality of solvents. It was observed in several simulations[7,13] and experimental studies of dendrimer systems.[8] However, our results confirm that eqs 4 and 5 are the correct scaling laws.

It is somewhat surprising that the power law is followed even for small P in our simulations. It might attribute to the potential model, eq 7, we adopted. It is similar to the bond-fluctuation lattice model, in which a linear chain is rather stiff and reaches the scaling regime at relatively smaller N. Moreover, the long spacer condition is to avoid the effect associated with the detailed structure near the branching point. A freely jointed bond, which is allowed to fluctuate freely within a certain range, somehow fulfill this purpose. The success of the Flory-type theory for a linear branch is also remarkable. It is generally believed that side branches give additional elastic energy and correlation in the repulsive energy. Nevertheless, a correct scaling may result from a cancellation of two errors, which is the case for a linear chain.[2]

Many technological applications for starburst require a hollow interior. The structure can be characterized by the mean volume fraction ($\sim N^{2/5}/[(g + 1)P]^{6/5}$) and the ratio R_e/R_g. The qualitative features of the latter based on simulations agree with those of a phantom chain: $R_e/R_g \geq 1$ and independent of P. As the generation number increases, the density rises and R_e/R_g declines toward 1. The branches are forced to fold back. This result indicates that one is unable to attain a dense shell with a solvent-filled hollow core simply by increasing the generation number.

Acknowledgment. H.-K.T. thanks NSC of Taiwan for financial support, and S.J. gratefully acknowledges NSF for a Career Award.

References and Notes

(1) Tomalia, D. A.; Naylor, A. M.; Goddard III W. A. *Angew. Chem., Int. Ed. Engl.* **1990**, *29*, 138. Bosman, A. W.; Janssen, H. M.; Meijer, E. W. *Chem. Rev.* **1999**, *99*, 1665.
(2) de Gennes, P.-G. *Scaling Concepts in Polymer Physics*; Cornell University Press: Ithaca, NY, 1979. Grosberg, A. Y.; Khokhlov, A. R. *Statistical Physics of Macromolecules*; AIP: New York, 1994.
(3) de Gennes, P.-G.; Hervet, H. *J. Phys., Lett.* **1983**, *44*, L351.
(4) Lescanec, R. L.; Muthukumar, M. *Macromolecules* **1990**, *23*, 2280.
(5) Mansfield, M.; Klushin, L. *Macromolecules* **1993**, *26*, 4262.
(6) Chen, Z.-Y.; Cui, S.-M. *Macromolecules* **1996**, *29*, 7943.
(7) Murat, M.; Grest, G. S. *Macromolecules* **1996**, *29*, 1278.
(8) Scherrenberg, R.; Coussens, B.; van Vliet, P.; Edouard, G.; Brackman, J.; de Brabander, E. *Macromolecules* **1998**, *31*, 456. Stechemesser, S.; Eimer, W. *Macromolecules* **1997**, *30*, 2204.
(9) Boris, D.; Rubinstein, M. *Macromolecules* **1996**, *29*, 7251.
(10) La Ferla, R. *J. Chem. Phys.* **1997**, *106*, 688.
(11) Zhou, Y.; Hall, C. K.; Karplus, M. *Phys. Rev. Lett.* **1996**, *77*, 2822.
(12) Yong, C. W.; Clake, J. H. R.; Freire, J. J.; M. Bishop, *J. Chem. Phys.* **1996**, *105*, 9666.
(13) Karatasos, K.; Adolf, D. B.; Davies, G. R. *J. Chem. Phys.* **2001**, *115*, 5310.

MA025561K